

Bending ratcheting behavior of pressurized straight Z2CND18.12N stainless steel pipe

Lei Wang¹, Gang Chen^{*1}, Jianbei Zhu¹, Xiuhu Sun¹, Yunhui Mei³, Xiang Ling²
and Xu Chen¹

¹School of Chemical Engineering and Technology, Tianjin University, 300072, China

²Jiangsu Key Laboratory of Process Enhancement & New Energy Equipment Technology,
NanJing University of Technology, 210009, China

³Tianjin Key Laboratory of Advanced Joining Technology and School of Material Science and Engineering,
Tianjin University, 300072, China

(Received October 7, 2013, Revised July 1, 2014, Accepted July 2, 2014)

Abstract. The ratcheting effect greatly challenges the design of piping components. With the assistance of the quasi-three point bending apparatus, ratcheting and the ratcheting boundary of pressurized straight Z2CND18.12N stainless steel pipe under bending loading and vertical displacement control were studied experimentally. The characteristics of progressive inelastic deformation in axial and hoop directions of the Z2CND18.12N stainless steel pipes were investigated. The experiment results show that the ratcheting strain occurs mainly in the hoop direction while there is less ratcheting strain in the axial direction. The characteristics of the bending ratcheting behavior of the pressure pipes were derived and compared under load control and displacement control, respectively. The results show that the cyclic bending loading and the internal pressure affect the ratcheting behavior of the pressurized straight pipe significantly under load control. In the meantime, the ratcheting characteristics are also highly associated with the cyclic displacement and the internal pressure under displacement control. All these factors affect not only the saturation of the ratcheting strain but the ratcheting strain rate. A series of multi-step bending ratcheting experiments were conducted under both control modes. It was found that the hardening effect of Z2CND18.12N stainless steel pipe under previous cyclic loadings no matter with high or low displacement amplitudes is significant, and the prior loading histories greatly retard the ratcheting strain and its rate under subsequent loadings. Finally, the ratcheting boundaries of the pressurized straight Z2CND18.12N stainless steel pipe were determined and compared based on KTA/ASME, RCC-MR and the experimental results.

Keywords: ratcheting; cyclic loading; cyclic displacement; loading history; ratcheting boundary

1. Introduction

Pressurized pipes are subjected to bending loads due to thermal expansion and shocks induced from sudden opening and closing of relief valves (Jahanian 1997). Under such kind of loading state, they usually suffer cyclic plastic accumulation, namely ratcheting, which can result in reduced fatigue life (Rider *et al.* 1995, Xia *et al.* 1996, Hassan *et al.* 1998, Kwofie 2006, Kang

*Corresponding author, Associate Professor, E-mail: agang@tju.edu.cn

2008, Shariati *et al.* 2012, Chen *et al.* 2013). The ratcheting behavior had been extensively studied, and it was found that the ratcheting strain evolution was greatly dependent on many factors, such as stress level (Kang and Liu 2008, Lin *et al.* 2013), loading history (Lin *et al.* 2013), stress rate (Li *et al.* 2013), loading path (Liu *et al.* 2010) and temperature (Kang *et al.* 2002), etc. However, the ratcheting of pressurized piping components belongs to structural ratcheting, which is more sophisticated than material ratcheting for its inhomogeneous multiaxial stress state due to various load combinations (Dang Van and Moumni 2000, Chen *et al.* 2013). In these cases, the pressure is considered to be the primary load and other loads are regarded as the secondary cyclic ones. Although the cost of operation is low, that of the in-service failure of pipelines is very high in terms of both economy and environment. Hence it is very important to research the characteristic of the ratcheting behavior of the pipelines in depth. In fact, the ratcheting effect had already been taken into account in many design criteria for engineering components and structures, including RCC-MR (2007), ASME Code Section III (2010) and KTA (2010).

The investigation on the pressurized pipes has aroused the widespread attention in the last several decades. Yoshida *et al.* (1984) studied mechanical ratcheting in a carbon steel pipe under combined cyclic axial load and steady internal pressure. It was found that the effects of maximum effective stress, stress ratio and steady stress affected the biaxial strain accumulation. Moreton *et al.* (1996) researched the onset of ratcheting in a pressurized piping elbow, which was subjected to in-plane bending moment. They determined the value of the bending moment necessary to initiate ratcheting in the elbow. Zakavia *et al.* (2010) described the ratcheting behavior of pressurized plain pipe subjected to cyclic bending moment with a combined hardening model. Wolters *et al.* (1997) investigated the ratcheting phenomena under different bending loads. The experimental results showed that the effect of a constant primary load in conjunction with a cyclic thermal loading on ratcheting was much more critical than that of a impact primary load. Krämer *et al.* (1997) researched the ratcheting behavior of austenitic pipes and proposed an extension on isotropic hardening rule. Weiß *et al.* (2004) studied the combined ratcheting and low cycle fatigue damage mechanisms of welded and non-welded pressure vessel components. Rider *et al.* (1994) revealed that both stainless steel and low carbon steel pipes were satisfied with the proposed ASME standard, i.e., ratcheting strain limit of 5% hoop strain after 10 cycles of 1% axial strain range, no matter what the value of internal pressure was. So far, most of the ratcheting experiments of internal pressurized pipes had been carried out under load control, while only a few studies were performed on the characteristic of the bending ratcheting behavior under displacement control (Vishnuvardhan *et al.* 2010, Vishnuvardhan *et al.* 2013). Since the in-service pipes are usually constrained by the surrounded structures and subjected to a cyclic thermal stress induced from thermal deformation, it is necessary to investigate the bending ratcheting behavior of the internal pressurized pipes under displacement control, in which the loading conditions are quite similar to those in applications.

The ratcheting boundary is an essential criterion for piping design. Early in 1960s, the ratcheting boundary was firstly investigated by Bree (1967, 1989) (for a pressurized cylinder with a cyclic thermal stress across the wall thickness). Bree's results contributed to the formation of the ratcheting design standards in ASME and KTA. The efficiency diagram rule in RCC-MR, which was developed at the Centre d'Etudes Nucleaires in France, is an alternative rule to assure the ratcheting shakedown taking place. The Committee of Three Dimensional Finite element stress evaluation (C-TDF) in Japan proposed two alternative standards for shakedown analysis, in which an elastic perfect plasticity (EPP) model or a bilinear kinematic hardening rule was used (Asada *et al.* 2002, Yamamoto *et al.* 2002). Gao *et al.* (2006) studied the ratcheting and ratcheting boundary

Table 1 Main chemical composition of Z2CND18.12N stainless steel (wt. %)

C	Cr	Ni	Si	Mn	S	P	B	Mo	Cu	Co	N
0.025	17.517	12.073	0.430	1.221	0.003	0.021	0.001	2.388	0.075	0.035	0.070

of pressurized straight low carbon steel pipe under reversed bending. The ratcheting boundaries determined by the KTA/ASME, RCC-MR and C-TDF with a modified Jiang-Sehitoglu model were compared with the experimental results. It was shown that the ratcheting boundary determined by the C-TDF method divided the shakedown region well. Oh and Kim (2010) studied elastic-plastic behaviors of pressurized tubes under a cyclic thermal stress. They obtained the explicit equations for various stress regimes representing elastic-plastic behaviors. Yao *et al.* (2004) deduced a Bree-type load diagram based on an EPP model for straight pipe under cyclic bending with constant axial tensile load, but their work was not suitable for pipes subjected to non-proportional load due to the neglect the hoop stress. In practical work, the ratcheting standards stemming from the Bree's results are widely accepted (Ng and Nadarajah 1996) and applied to straight pressurized piping under cyclic thermal loads. However, pressurized piping does endure quite different types of the loading rather than pressure vessel. Cyclic thermal loading leads not only cyclic through-wall thermal stress, but also cyclic uniform axial or bending stress in piping components due to the extension or compression of the piping system. Therefore, it is important to investigate the ratcheting boundary of the practical pressurized pipe to enrich or modify the existed standards and serve for the practical work.

In this paper, bending ratcheting experiments under displacement control and load control were conducted. The pressurized straight pipe of Z2CND18.12N stainless steel, which was used in pressurized water reactor of nuclear power plants, was studied to understand its bending ratcheting behavior. A simplified ratcheting boundary was proposed based on the experimental tests.

2. Material properties and details of experiment

2.1 Pipe material and specification

The material of the straight internal pressurized pipe used in this study is austenitic stainless steel Z2CND18.12N (in French materials designation). The main chemical compositions of the material are shown in Table 1. The specimen is like a dumbbell type with gage sections of 10mm in diameter and 25mm in axial length. In order to characterize the bending ratcheting behavior of the pressurized pipe clearly, the monotonic tensile test was firstly conducted on MTS810 testing machine with a constant strain rate of 1×10^{-3} /s at room temperature. Some basic tensile properties, such as yield strength (266MPa), ultimate strength (590MPa) and the Young's modulus (195GPa), etc. were obtained. The relationship between strain and stress of the material is shown in Fig. 1.

The pipe specimen used in bending ratcheting experiment is Z2CND18.12N stainless steel pipe with an outside diameter of 76 mm, a thickness of 4.5 mm and a length of 1200 mm. In order to withstand the internal pressure, we welded the specimen with two circular plates of Z2CND18.12N stainless steel with a thickness of 6 mm and a diameter of 76 mm at each end.

2.2 Testing apparatus

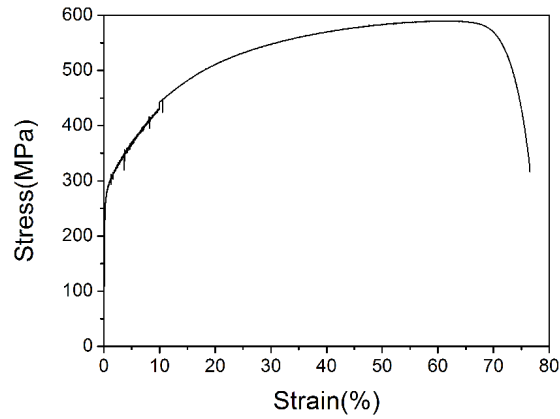
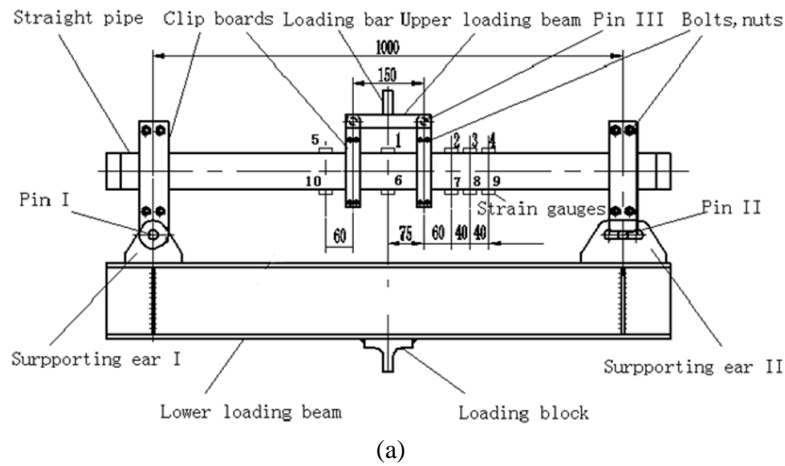


Fig. 1 Stress-strain curve of monotonic uniaxial tension



(a)



(b)

Fig. 2 The quasi-three point bending apparatus (a) profile drawing where the numbers 1-10 refer to the locations of attached strain gauges; (b) actual picture

The tests were conducted on a 100-kN closed-loop servo-hydraulic multiaxial fatigue testing machine with a digital controller. The apparatus is capable of applying axial load and internal pressure independently or synchronously. The digital control system was developed by CARE

Measure & Control Co., Ltd. (CARE Measure & Control Co.).

The profile drawing and the actual picture of the quasi-three point bending setup are shown in Fig. 2. The piping specimen is supported on the lower loading beam, which is composed of supporting ears, clip boards, pins, bolts and nuts. The upper loading beam is connected to the specimen with clip boards, pins, bolts and nuts. Both the loading bar screwed into the upper loading beam and the loading block welded on the lower loading beam are clamped in the hydraulic clip of the testing machine. Thin walled pipes are in bi-axial stresses states due to the effect of internal pressure, while the bending stresses are applied on the pipes in the axial direction to achieve a non-proportional multi-axial loading condition. In order to record the ratcheting strains, ten bi-axial strain gauges are adhered on the specimen aligned to the axial and the hoop direction. The strain gauges are assigned to the positions presented in Fig. 2(a). The values of loading, strain, pressure and time are simultaneously recorded by a computer-controlled data acquisition system.

2.3 Details of experiment

The characteristics of progressive inelastic deformation of straight pressurized pipe under different constant pressures, different controlled cyclic displacements or cyclic bending loadings were investigated. To study the effect of the control mode, the bending ratcheting tests were performed under load control and displacement control, respectively. A series of multi-step bending ratcheting experiments were conducted under both control modes to study the influence of the bending history. The details of the experimental conditions are shown in Table 2 and Table 3. For all tests, the controlled wave form of load or displacement was symmetrical triangular and each loop cycle was 30 seconds. In this study, the ratcheting strain is defined as the mean strain in a cycle (Ohno 1997)

$$\varepsilon_r = \frac{1}{2}(\varepsilon_{\max} + \varepsilon_{\min}) \tag{1}$$

where, ε_{\max} and ε_{\min} are the maximum and minimum strain in a cycle.

Table 2 Experimental conditions of Z2CND18.12N stainless steel pipes under bending load control

Spec. No.	Loading step	Internal Pressure (MPa)	Bending load (kN)	Number of cycles
12NSR5	1	17.5	25	500
	2	20	25	50
	3	20	30	50
	4	20	35	30
12NSR6	1	20	30	500
	2	17.5	30	20
	3	20	35	50
12NSR7	1	20	35	500
12NSR8	1	23	30	300
12NSR9	1	26	35	15
	2	20	35	20

Table 3 Experimental conditions of Z2CND18.12N stainless steel pipes under displacement control

Spec. no.	Loading step	Internal Pressure (MPa)	Vertical displacement (mm)	Number of cycles
12NSR1	1	20	5	150
	2	20	5.5	35
	3	20	6	35
12NSR2	1	17.5	6	150
	2	20	6	35
	3	23	6	35
	4	17.5	6	35
	5	25	6	35
12NSR3	1	17.5	5	150
	2	17.5	6	35
	3	17.5	7	35
	4	17.5	5	35
	5	17.5	7	35
	6	17.5	7.5	35
12NSR4	1	20	6	220
	2	20	5	35
	3	20	6	35
	4	20	7	35
	5	20	6	35

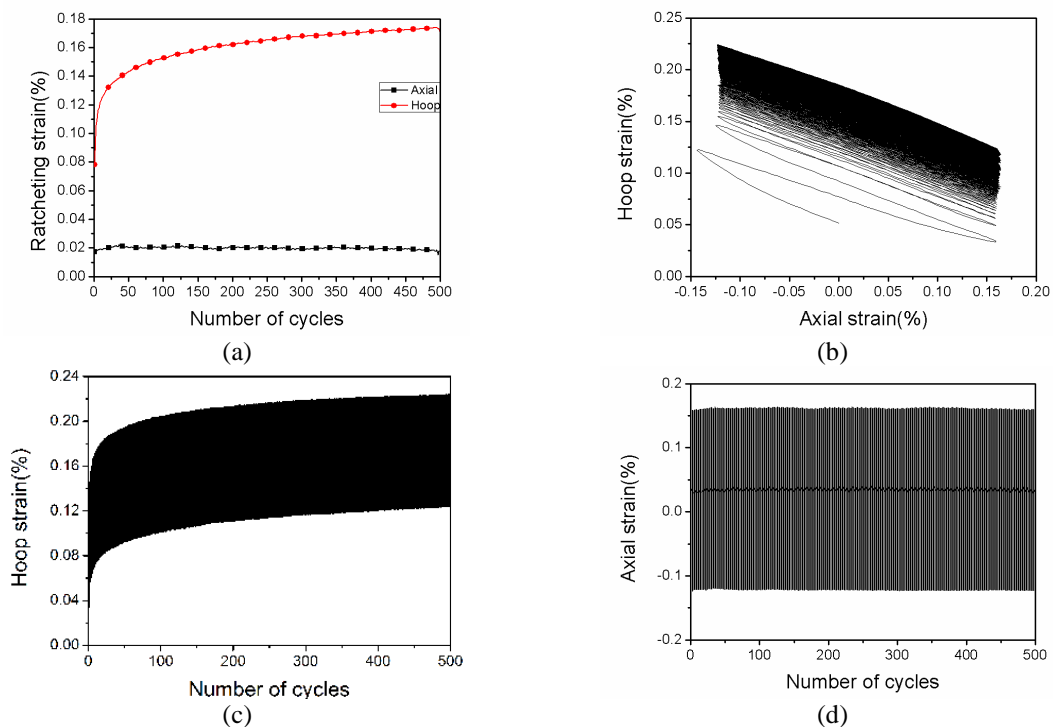


Fig. 3 Results of the bending ratcheting tests: (a) Ratcheting strain at position 6 versus the number of cycles; (b) Axial strain versus hoop strain at position 6; (c) Hoop strain at position 6 versus the number of cycles; (d) Axial strain at position 6 versus the number of cycles; (e) Ratcheting strain at each typical position versus the number of cycles

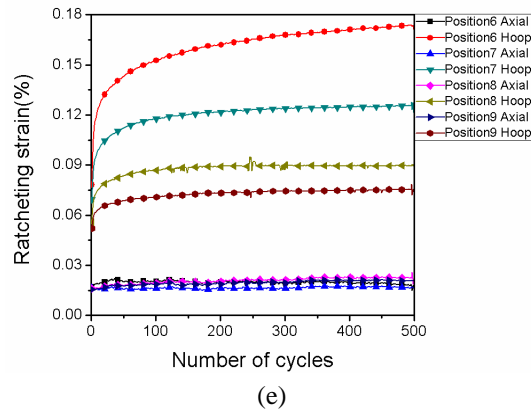


Fig. 3 Continued

3. Results and discussion

3.1 Bending ratcheting behavior under load control

To present the characteristics of the bending ratcheting behavior of pressurized straight Z2CND18.12N stainless steel pipes under cyclic bending load, the results of the first step of 12NSR5 are shown in Fig. 3. The loading condition is 17.5 MPa and ± 25 kN. Based on the results, it can be discerned clearly that the bending ratcheting strain does occur at various tested positions during the first 500 cycles. More specifically, the amplitude and the change of the hoop ratcheting strain are much larger than that of the axial direction because of the larger mean stress. The axial stress is derived from the constant internal pressure and the cyclic bending load, but the hoop stress is mainly generated from the constant internal pressure. Although the peak axial stress is larger than that in the hoop direction, which leads to a larger axial strain amplitude, the hoop stress is one time larger than axial stress derived from the same internal pressure, which means the mean stress in hoop direction is one time larger than that in axial direction. Therefore, the plastic strain is mainly accumulated in the hoop direction but not evident in the axial direction. In addition, all of the hoop ratcheting strains at various positions experience a dramatically upward trend in the first 30 cycles, then decrease significantly with the number of cycles and reach a steady stage where the increase of the ratcheting strain and its rate are relatively small. Similar observations were also obtained in many other materials and structures (Kang 2008, Chen *et al.* 2013, Lin *et al.* 2013).

The Comparisons all of the hoop ratcheting strain at each position are shown in Fig. 3(e). It is obviously that the ratcheting strains at various positions are quite different from each other. The most noteworthy ratcheting strain is recorded at the center of the pipe. The strain becomes small with increasing in a distance far from the centerline of pipe. The hoop ratcheting strain and its rate are also largest in the middle comparing with other positions. Though the stress derived from a constant internal pressure is equal at each position, the moment caused by the bending load is much larger at the center position than those away from the center. Moreover, the hoop ratcheting strain at position 6 (shown in Fig. 2(a)) increases without shakedown in the range of tested cycles while the hoop ratcheting strains at other positions nearly shakedown after only 50 cyclic loadings.

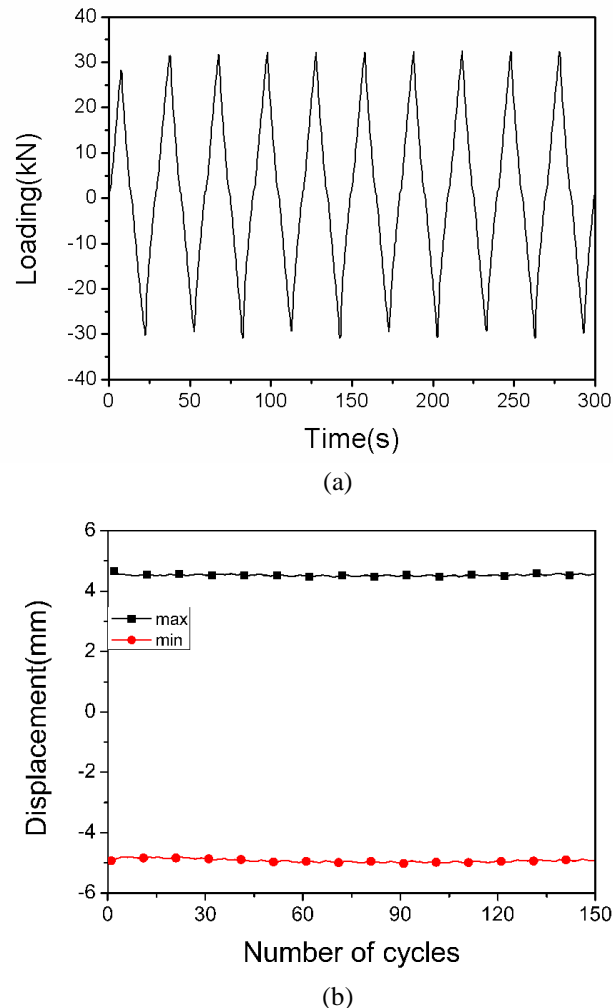


Fig. 4 Cyclic displacement response of 12NSR6 under load control: (a) Load versus time in the first 10 cycles; (b) peak displacement versus number of cycles

3.2 Comparison of the bending ratcheting behaviors under different control modes

Fig. 4(a) indicates the relationship of the displacement versus time of 12NSR6 under load control mode, and the maximum and minimum displacement of each cycle versus the number of cycles is shown in Fig. 4(b). It can be seen clearly that the displacement amplitude in the first cycle is much larger than that in the following cycles. The internal pressurized pipe shows a quickly hardening trend in the first cycle under load control mode. Moreover, after the first cycle the maximum and minimum displacement is around 5mm and -5mm, respectively. Therefore, the cyclic test of internal pressurized pipe under displacement control was conducted under the displacement of ± 5 mm and the constant internal pressure (12NSR1).

The bending loading response of 12NSR1 under displacement control mode is plotted in Fig. 5. It can be seen that the displacement amplitude in the first cycle is much larger than that in the

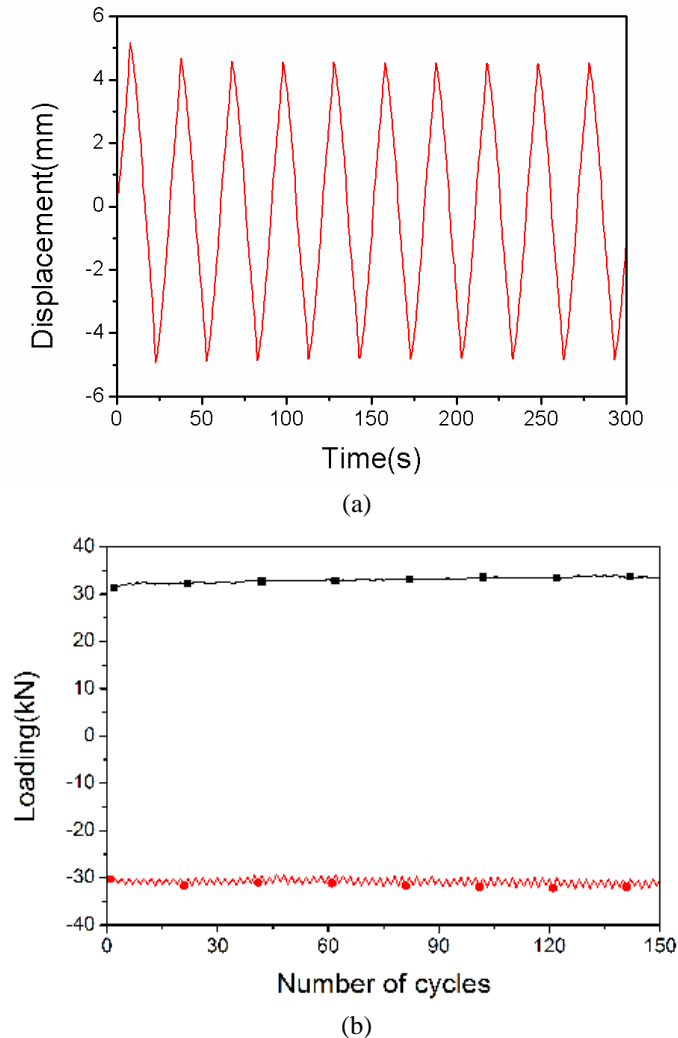


Fig. 5 Cyclic load response of 12NSR1 under displacement control: (a) displacement versus time in the first 10 cycles; (b) peak load versus number of cycles

following cycles because of the controlling overshoot. The internal pressurized pipe also shows a quickly hardening trend in the first cycle under the displacement control, which is highly similar with the trend under load control. Moreover, the maximum and minimum loading after the first cycle is around 30kN and -30kN, respectively.

Then, the ratcheting strain responses at each position under displacement control (12NSR1) and load control (12NSR6) modes are obtained and compared in Fig. 6. Fig. 7 shows the relationship between the bending moment and the hoop ratcheting strain at position 6. Comparing the ratcheting strain at each position under different control modes, it is obvious that the ratcheting strain under the displacement control is similar with that under the load control mode, though the ratcheting strain under the displacement control at position 6 and position 7 is a little larger than that under the load control. This is because the bending loading under displacement control is a bit

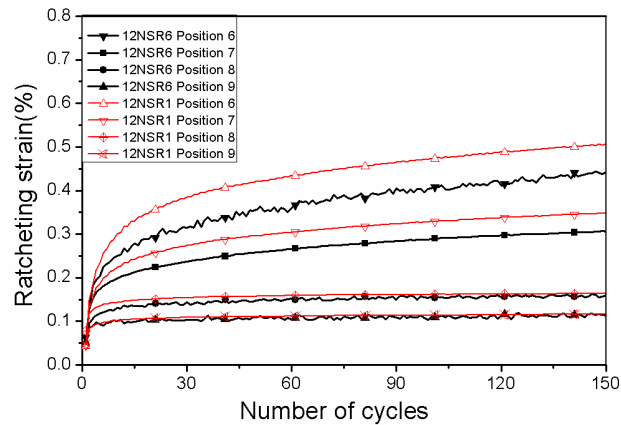


Fig. 6 Ratcheting strain at each position under displacement and load control modes

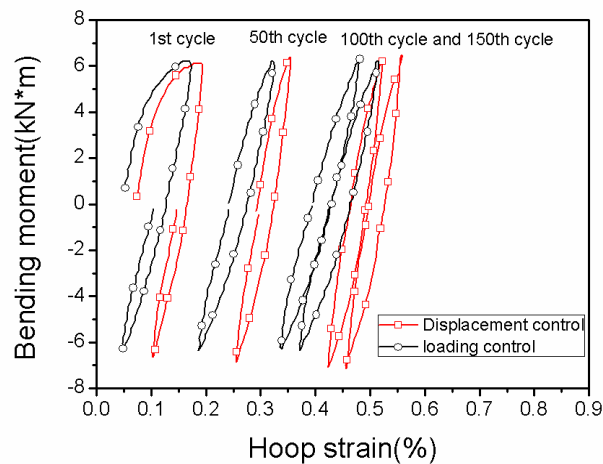


Fig. 7 Bending moment versus hoop strain at position 6

higher than that of 12NSR6 under load control. Moreover, it is obvious that the displacement response is almost the same with that under displacement control mode after the first cycle according to Fig. 4 (a), while the bending loading response under the displacement control is also the same with that under the load control mode after the first cycle as shown in Fig. 5 (a). Therefore, it can be concluded that the control mode influences the characteristics of the bending ratcheting behavior slightly and there may be only some differences in the first cycle of the ratcheting strain under different control modes. In addition, the ratcheting behavior under load control can be used to forecast the characteristics of the ratcheting behavior under displacement control and vice versa.

3.3 Ratcheting behavior under different internal pressures

Two different internal pressures tests under load control (12NSR6 and 12NSR8) and displacement control (12NSR1 and 12NSR3) were conducted to investigate the effect of the

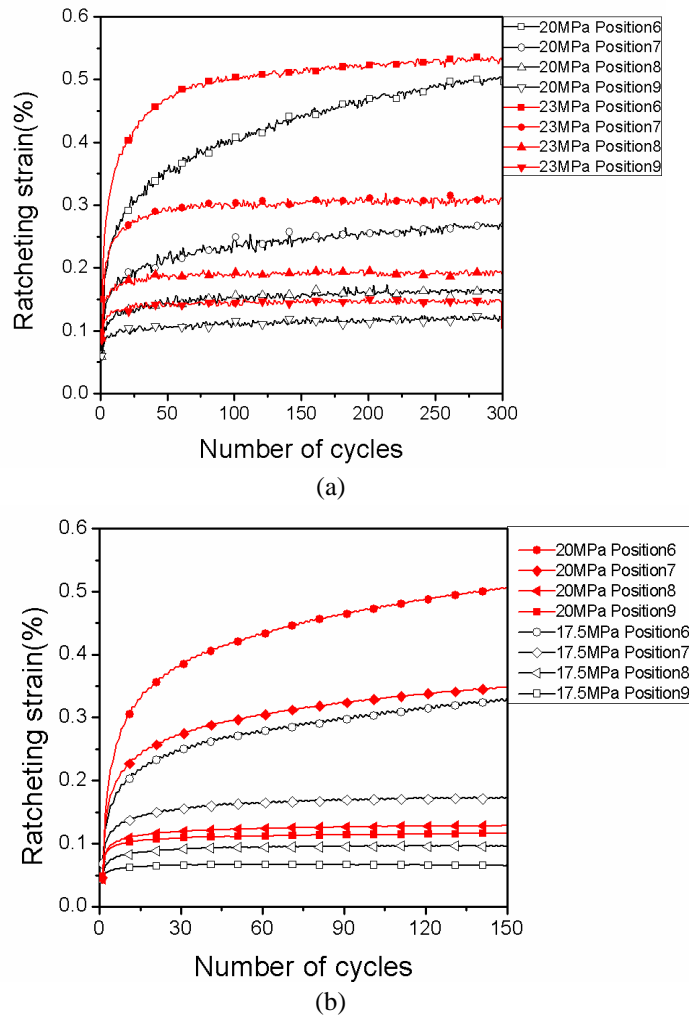


Fig. 8 Hoop ratcheting strain under different internal pressures: (a) with the same bending load; (b) with the same vertical displacement

internal pressure on the ratcheting behavior. The hoop ratcheting strain evolution curves at each typical position are given in Fig. 8. It is clear from the plots that the internal pressure significantly affects the ratcheting strain rate. The higher the internal pressure, the higher rate of ratcheting strain accumulation for both control modes.

3.4 Ratcheting behavior under different axial loads or displacements

Fig. 9(a) shows the hoop ratcheting strains of 12NSR6 and 12NSR7 under load control at each typical position to present the impact of the controlled cyclic bending load on the ratcheting behavior. The hoop ratcheting strains of 12NSR2 and 12NSR3 at each typical position are given in Fig. 9(b) to describe the effect of the controlled cyclic displacement on the ratcheting behavior. It is revealed that the hoop ratcheting strain with a larger controlled cyclic bending load or vertical

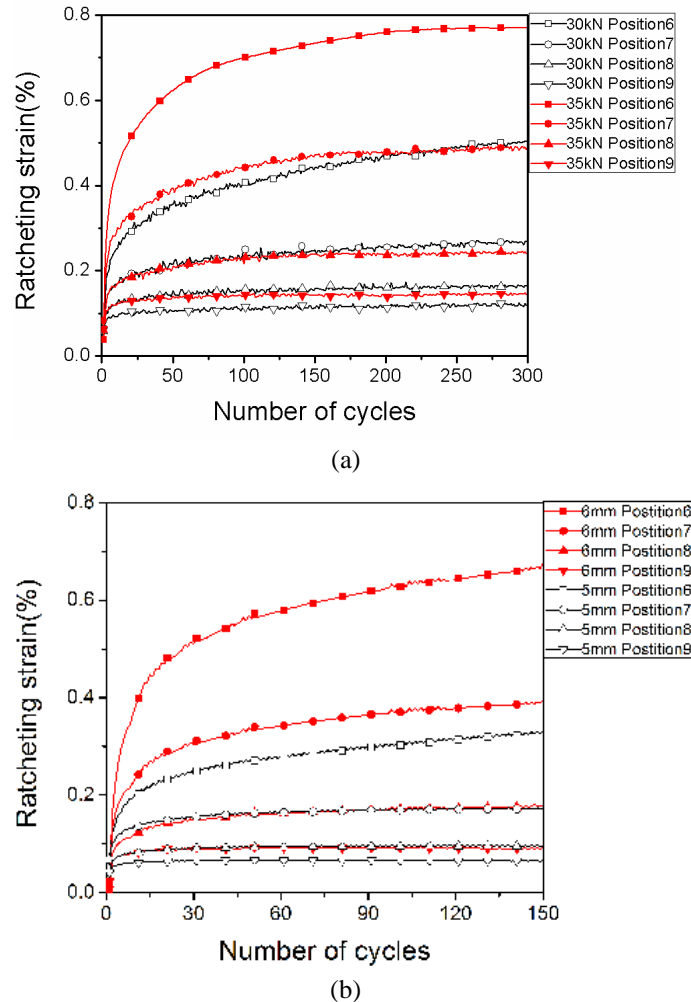


Fig. 9 Hoop ratcheting strain under different control modes with the same internal pressure (a) load control; (b) displacement control

displacement is much larger than that with a small one at the same position. In addition, the hoop ratcheting strain rate and the shakedown rate also increase with increasing in the controlled cyclic bending load or vertical displacement (namely the cyclic secondary loading).

3.5 Effect of the loading history on ratcheting behavior

3.5.1 Bending history under load control

Multi-step ratcheting tests with the various internal pressures and axial loads were carried out. Fig. 10 shows the ratcheting strain of 12NSR5 at each typical position under the multi-step loading conditions: ① 17.5 MPa, 25 kN; ② 20 MPa, 25 kN; ③ 20 MPa, 30 kN; ④ 20 MPa, 35 kN. The hoop ratcheting strain evolution of 12NSR6 at every typical position is given in Fig. 11, and the multi-step loading conditions are listed as: ① 20 MPa, 30 kN; ② 17.5 MPa, 30 kN; ③

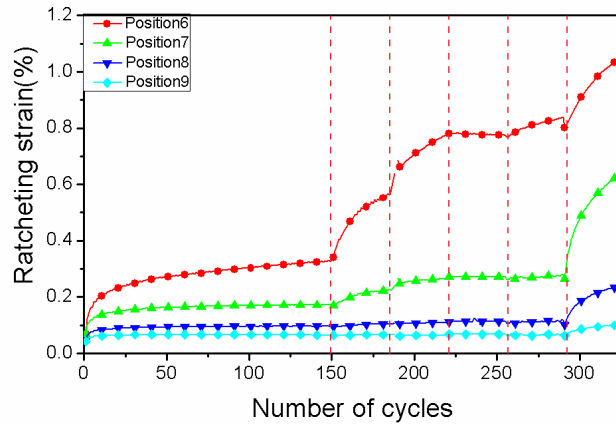


Fig. 10 Ratcheting strain versus number of cycles of 12NSR5

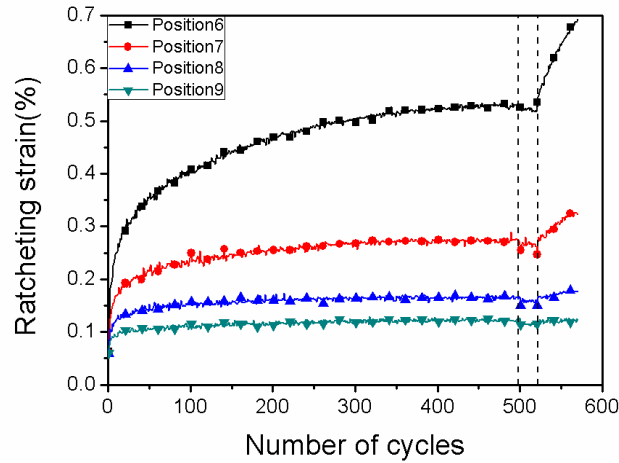


Fig. 11 Ratcheting strain versus number of cycles of 12NSR6

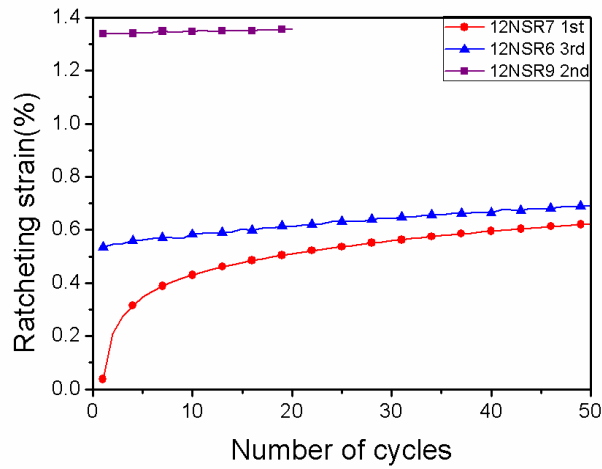


Fig. 12 Comparison of the ratcheting strain at position 6

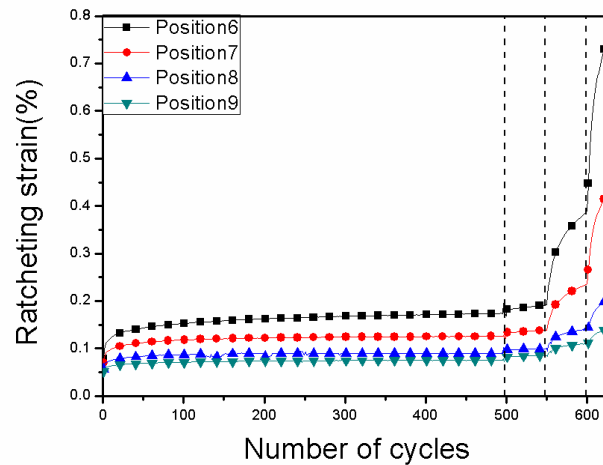


Fig. 13 Hoop ratcheting strain versus number of cycles of 12NSR3

20MPa, 35 kN. It is evident that the hoop ratcheting strain does occur at every position in each step according to the results. More specifically, the hoop ratcheting strain and its rate for every position increase significantly with the elevated bending loads or internal pressures.

In order to demonstrate the effect of the bending history on the ratcheting behavior, the ratcheting strains at position 6 with and without the bending history are compared and the results are shown in Fig. 12. The ratcheting strains of 12NSR6, 12NSR7 and 12NSR9 under the internal pressure of 20MPa and the cyclic load of 35 kN are compared. It can be clearly discerned that the bending history decreases the hoop ratcheting strain rate significantly. Comparing the hoop ratcheting strain of 12NSR7 in the first step with that of 12NSR6 in the third step, it can be found that the ratcheting strain reaches nearly the same level after 35 cycles though the hoop ratcheting strain rate of the former is larger than the latter. At the same time, the hoop ratcheting strain of 12NSR9 in step 2 is nearly zero, which means the loading history of cycling under a high internal pressure can restrain the ratcheting strain accumulation of subsequent cycling under a low pressure. The phenomena are in accordance with the observations on low carbon steel pipe performed by Gao *et al.* (2006).

3.5.2 Bending history under displacement control

Fig. 13 shows the hoop ratcheting strain at each typical position versus the number of cycles for a six-step multi-axial loadings. In this case, the constant internal pressure is maintained constant at 17.5 MPa, while the cyclic displacement amplitudes are 5 mm, 6 mm, 7 mm, 5 mm, 7 mm and 7.5 mm in step 1, 2, 3, 4, 5 and 6, respectively. In step 1, the ratcheting rate decreases with increasing in loading cycles, following a nonlinear relation in terms of the number of cycles. Due to the increase of displacement amplitude, the ratcheting rate in step 2 is higher than that in step 1, and there is a similar condition appeared in the following step 3. As the displacement amplitude decreases from 7 mm to 5 mm, the hoop ratcheting strain decreases and its accumulation direction is opposite to that of step 3, as shown in Fig. 13. When the displacement amplitude is increased to 7mm, the hoop ratcheting strain exhibits in a similar way as that appears in step 3, but it is much lower than expected compared to the case of step 3. In the last step, the ratcheting strain at each position increases noticeably when the controlled displacement amplitude changes to 7.5 mm.

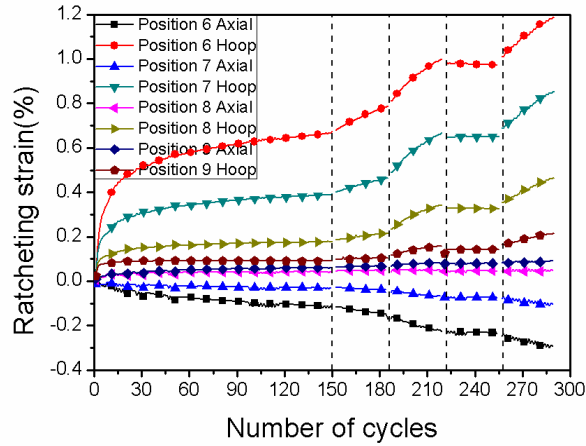
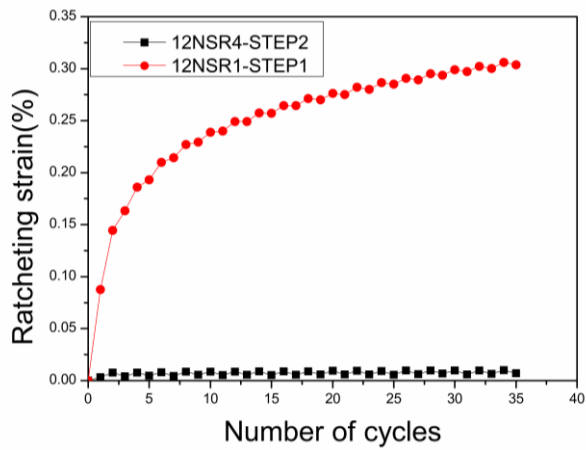
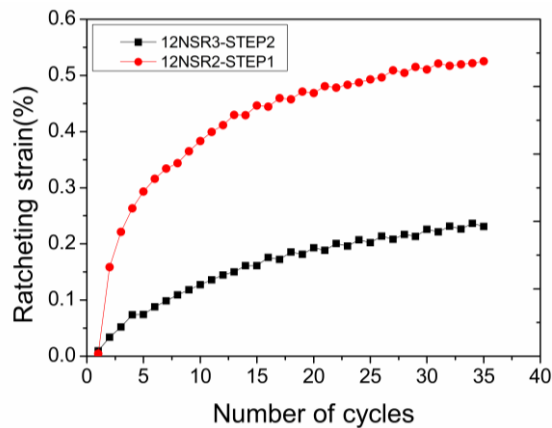


Fig. 14 Hoop ratcheting strain versus number of cycles of 12NSR2



(a)



(b)

Fig. 15 Comparison of hoop ratcheting strain versus number of cycles with and without loading history: (a) 12NSR1 step1 versus 12NSR4 step 2; (b) 12NSR2 step1 and 12NSR3 step2

Fig. 14 also presents the results obtained from the displacement-controlled cycling with variable internal pressures, the subsequence of loading history for internal pressures becomes low-high-low-high. A negative ratcheting strain rate appears at the beginning of step 4 and then reaches zero rapidly, which means the shakedown of ratcheting taken place in step 4. The above phenomena result from the enhancement of deforming resistance which is caused by the prior displacement-controlled cycling with a larger displacement or a higher internal pressure. This hardening effect retards the ratcheting of subsequent displacement cycling with smaller ones.

To make a further understand about the history effect on ratcheting for Z2CND18.12N stainless steel pipe, two sets of tests with prehistory loadings and isolated ones are compared and shown in Fig. 15, in which the hoop ratcheting strain at position 6 was plotted as a function of the number of cycles. In Fig. 15(a), one can see that shakedown appears at the second step of 12NSR4, which implies that the prior loading history with larger cyclic displacement amplitude significantly restrains the ratcheting strain of subsequent loading conditions as mentioned above. From Fig. 15(b), it is interesting to find that the ratcheting strain and its rate of subsequent cycling with a large displacement amplitude of 6mm does change a lot even though the prior cyclic loading with a small displacement (5 mm). It can be concluded that the hardening effect of Z2CND18.12N stainless steel pipe under previous cyclic loading no matter with high or low displacement amplitude is significant and can not be ignored.

Fig. 16 shows the relationship of the hoop ratcheting strain rate at position 6 versus the number of cycles with and without loading history under a cyclic displacement amplitude of 6 mm and an internal pressure of 20 MPa. For 12NSR4, the ratcheting strain rate decreases with increasing in loading cycles. After about 20 cycles, due to the increase of cyclic hardening effect, the rate of ratcheting strain accumulation slows down and it seems to ratchet under a constant ratcheting strain rate of 4.5×10^{-4} /cycle. It is clear that the ratcheting does not shakedown. However, the ratcheting strain rate evolution curves of 12NSR4 in step 3 and step 5 indicate that shakedown of the pipe occurred. It means the pipe has memorized the previous loading history, which in turn affects its strain evolution rule under the subsequent loadings. From Fig. 16, it can be also figured out that the ratcheting strain rate drops rapidly for those pipes subjected to prior cyclic loading

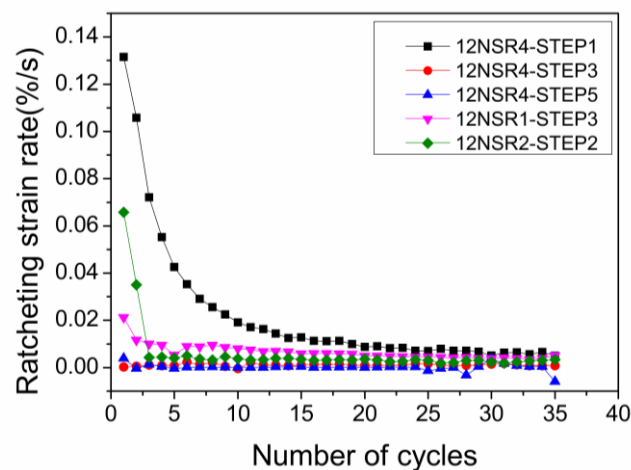


Fig. 16 The relationship of the hoop ratcheting strain rate versus number of cycles with and without the loading history

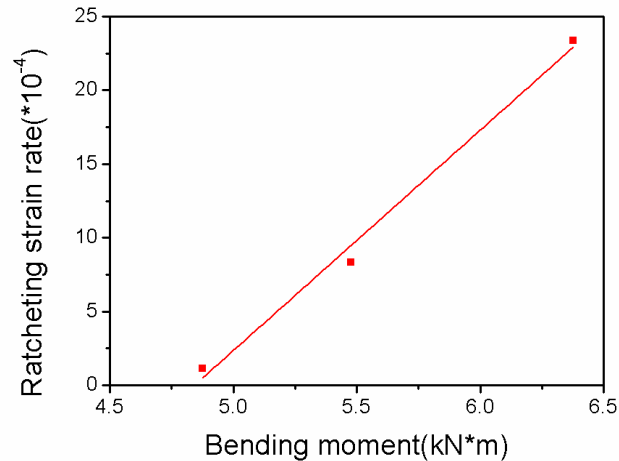


Fig. 17 Ratcheting strain rate versus bending moment

with small displacements or internal pressures, the ratcheting strains accumulation of 12NSR1 in step 3 and 12NSR2 in step 2 are much slower than that without loading history, which verified that the previous small loading history also retards the ratcheting behavior. It is worth noting that ratcheting strain rate of 12NSR1 in step 3 and 12NSR2 in step 2 is a little larger than those of 12NSR4 in step 3 and step 5, which means the hardening effect of prior small loading history is not strong enough to drive the pipes to shakedown.

3.6 Ratcheting boundary determination

3.6.1 Ratcheting boundary with regard to the internal pressure and the bending moment

According to the hoop ratcheting strains at various positions shown in Fig. 3(e), it is evident that the hoop ratcheting strains rate at different positions are different from each other. The quasi-three point bending apparatus was used to provide different bending loads (namely different moments) at various positions. With the assistance of this advantage, the ratcheting boundary point under a constant internal pressure can be determined by the ratcheting rate at various positions for different bending loads. For example, the ratcheting strain rate in the steady stage at each position of 12NSR6 can be obtained according to the experimental results. Then, the relationship of the ratcheting strain rate versus the moment under the internal pressure of 20 MPa could be plotted in Fig. 17. After that, the best fit straight line is obtained by a regression technique. Then find the intersection of the straight line and zero ratcheting strain line and take the corresponding moment as the ratcheting boundary point. In this way, all of the ratcheting boundary points could be achieved at different internal pressures. A ratcheting boundary, with regard to the internal pressure and the bending moment, can be determined following this method and shown in Fig. 18.

3.6.2 Comparison of the ratcheting boundaries

The ratcheting boundary for a pressurized pipe under a reversed bending load can be determined by KTA/ASME code, efficiency diagram rule of RCC-MR. For an arbitrary component geometry and load but without secondary peak stresses, a formula, which was adopted

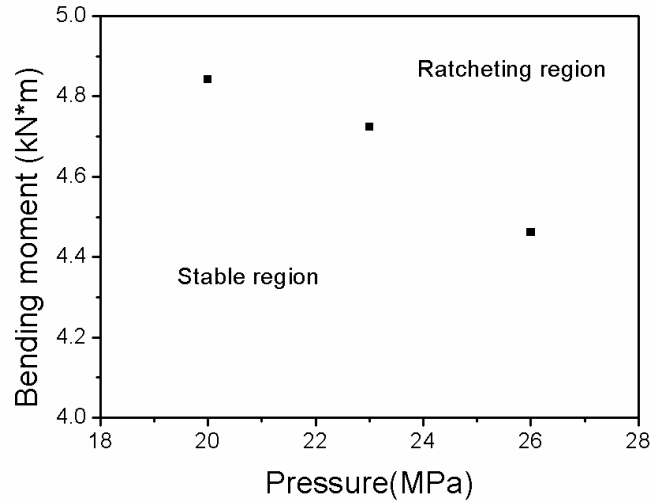


Fig. 18 Ratcheting boundary from the experimental results

by KTA and ASME standards, is used here to calculate the ratcheting boundary

$$\text{While } X \leq 1.0, \quad Y = 3.25(1 - X) + 1.33(1 - X)^3 + 1.38(1 - X)^5 \quad (2)$$

with the following definition

$$X \equiv \frac{P_m}{S_y} \quad (3)$$

$$Y \equiv \frac{\Delta Q}{S_y} \quad (4)$$

where, P_m is primary membrane stress; ΔQ is secondary stress range; S_y is yield stress.

For a thin walled straight pipe under internal pressure, its primary membrane stress is

$$P_m = \frac{KP}{K - 1} \quad (5)$$

where, K is the ratio of outer and inner diameter of the pipe. Therefore

$$X = \frac{KP}{(K - 1)S_y} \quad (6)$$

Under bending load ΔF , the secondary stress of the pipe is

$$\Delta Q = \frac{8\Delta F(l_0 - l_1)D_o}{\pi(D_o^4 - D_i^4)} \quad (7)$$

where, D_o and D_i are outer and inner diameter of the pipe, l_0 and l_1 are the spans of the lower and upper clips in Fig. 2(a). Thus

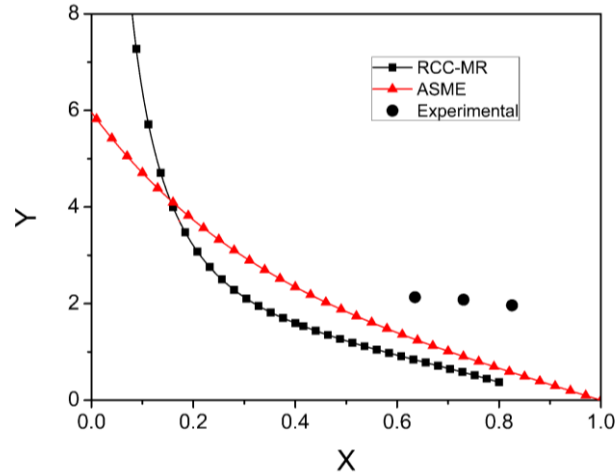


Fig. 19 Comparison of the ratcheting boundaries

$$Y = \frac{8\Delta F(l_0 - l_1)D_o}{\pi(D_o^4 - D_i^4)S_y} \tag{8}$$

The ratcheting boundary by ASME is shown in Fig. 19, in which the experimental data are also transformed into X and Y by Eqs. (7) and (8).

On the other hand, for the case of this study in which only the ratio of secondary stress and membrane stress are concerned, the ratcheting boundary can also be determined by RCC-MR. The method of Wolters (Yoshida *et al.* 1984) is used to transform the rules in RCC-MR into X and Y, defined in ASME as the following definitions

$$SR_1 = \frac{\Delta Q}{P_m} \tag{9}$$

$$v_1 = \frac{P_m}{1.2S_m} \tag{10}$$

Limitation against ratcheting is defined as

$$Y \leq 1.2v_1SR_1 \frac{S_m}{S_y} \tag{11}$$

where S_m is admissible stress.

Then, the correlations between the ratios of v_1 and SR_1 are determined

$$SR = \begin{cases} \frac{\sqrt{1.093-v}}{v-0.167} \times (\sqrt{1.093-v} + \sqrt{0.926}) & (1 \geq v \geq 0.5) \\ \frac{1}{v^2} & (0.5 \geq v \geq 0) \end{cases} \tag{12}$$

In fact, Eq. (12) is an implicit function of X and Y . The ratcheting boundary determined from it is shown in Fig. 19. Comparing all the ratcheting boundaries above, it is evident that both of the ratcheting boundaries obtained by KTA/ASME and RCC-MR are much more conservative than those derived from the experiments. In addition, the boundary curve of ASME allows a much higher range of secondary stress than that of RCCM-MR and approaches the experimental results better when $X \geq 0.53$ and vice versa.

4. Conclusions

With the assistance of the quasi-three point bending apparatus, ratcheting and the ratcheting boundary of pressurized straight Z2CND18.12N stainless steel pipe under load and displacement control were investigated experimentally. The impact of the control mode on the bending ratcheting strain was discussed. The characteristics of the ratcheting strain under different internal pressures, cyclic loadings and loading histories were compared. Finally, the ratcheting boundaries derived from ASME, RCC-MR and experiments were obtained. The following conclusions can be drawn:

- Accumulation of the strain was observed at every position both in the hoop and axial directions of the internal pressurized pipes under displacement and load control. However, the ratcheting strain occurs mainly in the hoop direction and the ratcheting strain rate in the hoop direction is also larger than that in the axial direction.
- The control mode influenced the characteristics of the bending ratcheting behavior slightly after the first cycle.
- The characteristics of the bending ratcheting behavior was affected by many factors, such as the internal pressure, cyclic displacement amplitude and cyclic loading amplitude, etc. The higher level of internal pressure or displacement (or bending loads), the larger ratcheting strain and its rate.
- The previous loading history greatly retarded the subsequent ratcheting behavior, the hardening effect of Z2CND18.12N stainless steel pipe under previous cyclic loading no matter with high or low displacement amplitude was significant and can not be ignored.
- The ratcheting boundaries obtained by KTA/ASME and RCC-MR tend to be more conservative than that of the experimental results. Actually, the boundary curve of ASME allows a much higher range of secondary stress than that of RCCM-MR and approaches the experimental results better when $X \geq 0.53$ and vice versa.

Acknowledgements

The authors gratefully acknowledge the financial support from the Jiangsu Key Laboratory of process enhancement & new energy equipment technology (No. 2013Z01) and Program for New Century Excellent Talents in University (NCET-13-0400), China.

References

Asada, S., Yamashita, N., Okamoto, A. and Nishiguchi, I. (2002), "Verification of alternative criteria for

- shakedown evaluation using flat head vessel”, *ASME 2002 Pressure Vessels and Piping Conference*.
- ASME (2010), “Boiler and ASME Pressure Vessel Code Section III: Rules for Construction of Nuclear Power Plant Components”, American Society of Mechanical Engineers, New York, NY.
- Bree, J. (1967), “Elastic-plastic behaviour of thin tubes subjected to internal pressure and intermittent high-heat fluxes with application to fast-nuclear-reactor fuel elements”, *J. Strain Anal. Eng. Des.*, **2**(3), 226-238.
- Bree, J. (1989), “Plastic deformation of a closed tube due to interaction of pressure stresses and cyclic thermal stresses”, *Int. J. Mech. Sci.*, **31**(11), 865-892.
- CARE Measure & Control Co., L. www.care-mc.com/index.html.
- Chen, X., Chen, X., Yu, D. and Gao, B. (2013), “Recent progresses in experimental investigation and finite element analysis of ratcheting in pressurized piping”, *Int. J. Pres. Ves. Pip.*, **101**, 113-142.
- Dang Van, K. and Moumni, Z. (2000), “Evaluation of fatigue-ratcheting damage of a pressurised elbow undergoing damage seismic inputs”, *Nucl. Eng. Des.*, **196**(1), 41-50.
- Gao, B., Chen, X. and Chen, G. (2006), “Ratchetting and ratchetting boundary study of pressurized straight low carbon steel pipe under reversed bending”, *Int. J. Pres. Ves. Pip.*, **83**(2), 96-106.
- Hassan, T., Zhu, Y. and Matzen, V.C. (1998), “Improved ratcheting analysis of piping components”, *Int. J. Pres. Ves. Pip.*, **75**(8), 643-652.
- Jahanian, S. (1997), “On the incremental growth of mechanical structures subjected to cyclic thermal and mechanical loading”, *Int. J. Pres. Ves. Pip.*, **71**(2), 121-127.
- Kang, G., Gao, Q., Cai, L. and Sun, Y. (2002), “Experimental study on uniaxial and nonproportionally multiaxial ratcheting of SS304 stainless steel at room and high temperatures”, *Nucl. Eng. Des.*, **216**(1), 13-26.
- Kang, G. and Liu, Y. (2008), “Uniaxial ratchetting and low-cycle fatigue failure of the steel with cyclic stabilizing or softening feature”, *Mat. Sci. Eng. A*, **472**(1), 258-268.
- Kang, G.Z. (2008), “Ratchetting: Recent progresses in phenomenon observation, constitutive modeling and application”, *Int. J. Fatigue*, **30**(8), 1448-1472.
- Krämer, D., Krolop, S., Scheffold, A. and Stegmeyer, R. (1997), “Investigations into the ratchetting behaviour of austenitic pipes”, *Nucl. Eng. Des.*, **171**(1), 161-172.
- KTA (2010), “Kerntechnischer Ausschuss (KTA), Sicherheitstechnische Regel des KTA; Komponenten des primärkreises von Leichtwasserreaktoren”, Teil: Auslegung, Konstruktion und Berchnung, Regeländerungsentwurf.
- Kwofie, S. (2006), “Cyclic creep of copper due to axial cyclic and tensile mean stresses”, *Mat. Sci. Eng. A*, **427**(1), 263-267.
- Li, S., Wang, H., Wang, Y., Wang, C., Niu, H. and Yang, J. (2013), “Uniaxial ratchetting behaviour of cerium oxide filled vulcanized natural rubber”, *Polym. Test.*, **32**(3), 468-474.
- Lin, Y., Chen, X.M., Liu, Z.H. and Chen, J. (2013), “Investigation of uniaxial low-cycle fatigue failure behavior of hot-rolled AZ91 magnesium alloy”, *Int. J. Fatigue*, **48**, 122-132.
- Lin, Y., Liu, Z.H., Chen, X.M. and Chen, J. (2013), “Stress-based fatigue life prediction models for AZ31B magnesium alloy under single-step and multi-step asymmetric stress-controlled cyclic loadings”, *Comp. Mater. Sci.*, **73**, 128-138.
- Lin, Y., Liu, Z.H., Chen, X.M. and Chen, J. (2013), “Uniaxial ratcheting and fatigue failure behaviors of hot-rolled AZ31B magnesium alloy under asymmetrical cyclic stress-controlled loadings”, *Mat. Sci. Eng. A*, **573**, 234-244.
- Liu, Y., Kang, G. and Gao, Q. (2010), “A multiaxial stress-based fatigue failure model considering ratchetting-fatigue interaction”, *Int. J. Fatigue*, **32**(4), 678-684.
- Moreton, D., Yahiaoui, K. and Moffat, D. (1996), “Onset of ratchetting in pressurised piping elbows subjected to in-plane bending moments”, *Int. J. Pres. Ves. Pip.*, **68**(1), 73-79.
- Ng, H. and Nadarajah, C. (1996), “Biaxial Ratcheting and Cyclic Plasticity for Bree-Type Loading-Part I: Finite Element Analysis”, *J. Press. Vess-T*, ASME, **118**(2), 154-160.
- Oh, C.S., Kim, Y.J. and Yoon, K.B. (2010), “Elastic-plastic behaviours of pressurised tubes under cyclic thermal stresses with temperature gradients”, *Int. J. Pres. Ves. Pip.*, **87**(5), 245-253.

- Ohno, N. (1997), "Recent progress in constitutive modeling for ratchetting", *Mater. Sci. Res.*, **3**(1), 1-9.
- Rider, R., Harvey, S. and Chandler, H. (1995), "Fatigue and ratcheting interactions", *Int. J. Fatigue*, **17**(7), 507-511.
- Rider, R., Harvey, S. and Charles, I. (1994), "Ratchetting in pressurised pipes", *Fatigue Fract. Eng. M.*, **17**(4), 497-500.
- RCC-MR (2007), "Design Rules for Class 1 Equipment", RB 3000.
- Shariati, M., Hatami, H., Torabi, H. and Epakchi, H.R. (2012), "Experimental and numerical investigations on the ratcheting characteristics of cylindrical shell under cyclic axial loading", *Struct. Eng. Mech.*, **44**(6), 753-762.
- Vishnuvardhan, S., Raghava, G., Gandhi, P., Saravanan, M., Goyal, S., Arora, P., Gupta, S.K. and Bhasin, V. (2013), "Ratcheting failure of pressurised straight pipes and elbows under reversed bending", *Int. J. Pres. Ves. Pip.*, **105**, 79-89.
- Vishnuvardhan, S., Raghava, G., Gandhi, P., Saravanan, M., Pukazhendhi, D., Goyal, S., Arora, P. and Gupta, S.K. (2010), "Fatigue ratcheting studies on TP304 LN stainless steel straight pipes", *Procedia Eng.*, **2**(1), 2209-2218.
- Weiß, E., Postberg, B., Nicak, T. and Rudolph, J. (2004), "Simulation of ratcheting and low cycle fatigue", *Int. J. Pres. Ves. Pip.*, **81**(3), 235-242.
- Wolters, J., Breitbach, G., Rüdiger, M. and Nickel, H. (1997), "Investigation of the ratcheting phenomenon for dominating bending loads", *Nucl. Eng. Des.*, **174**(3), 353-363.
- Xia, Z., Kujawski, D. and Ellyin, F. (1996), "Effect of mean stress and ratcheting strain on fatigue life of steel", *Int. J. Fatigue*, **18**(5), 335-341.
- Yamamoto, Y., Yamashita, N. and Tanaka, M. (2002). "Evaluation of thermal stress ratchet in plastic FEA", *ASME 2002 Pressure Vessels and Piping Conference*.
- Yao, Y., Lu, M.W. and Zhang, X. (2004), "Elasto-plastic behavior of pipe subjected to steady axial load and cyclic bending", *Nucl. Eng. Des.*, **229**(2), 189-197.
- Yoshida, F., Obataya, Y. and Shiratori, E. (1984), "Mechanical ratcheting behaviors of a steel pipe under combined cyclic axial load and internal pressure", *Society of Materials Science Proc. of the 27 th Japan Congr. on Mater. Res.*, 13-24 (SEE N 85-34180 23-23).
- Zakavi, S., Zehsaz, M. and Eslami, M. (2010), "The ratchetting behavior of pressurized plain pipework subjected to cyclic bending moment with the combined hardening model", *Nucl. Eng. Des.*, **240**(4), 726-737.